

Size effects on the phase coexistence in MnAs/GaAs(001) ribbons

M. Tortarolo,¹ M. Sirena,^{1,2} J. Milano,^{1,2,3} L. B. Steren,^{2,4} F. Vidal,³ B. Rache Salles,³ V. H. Etgens,³ M. Eddrief,³ G. Faini,⁵ and L. I. Pietrasanta^{2,6}

¹Centro Atómico Bariloche, CNEA, 8400 S. C. de Bariloche, Argentina

²Consejo Nacional de Investigaciones Científicas y Técnicas, C1033AAJ Buenos Aires, Argentina

³Institut des NanoSciences de Paris, CNRS UMR 7588, UPMC, 140 rue de Lourmel, 75015 Paris, France

⁴Centro Atómico Constituyentes, CNEA, 1650 San Martín, Argentina

⁵Phynano Team, Laboratoire de Photonique et de Nanostructures, CNRS, Route de Nozay, 91960 Marcoussis, France

⁶Centro de Microscopías Avanzadas, Facultad de Ciencias Exactas y Naturales, Universidad de Buenos Aires, Intendente Güiraldes 2160, C1428EHA Buenos Aires, Argentina

(Received 3 May 2010; published 2 June 2010)

Size and orientation effects on the phase coexistence in MnAs/GaAs(001) microribbons were studied using magnetic force microscopy. The magnetostructural phase coexistence reported in MnAs thin films is also observed in the microribbons, even in the smallest ones. However, the stripe array of MnAs films is only preserved in the ribbons confined along the [0001] direction. Nevertheless, the configuration of the magnetoelastic domains is altered in the ribbons confined along the [11 $\bar{2}$ 0] direction. In this last case, the micrometric ribbons exhibit a redistribution of the magnetoelastic phases owed to the relaxation of the epitaxial strains. The results are understood in terms of the anisotropic change in the lattice parameters at the magnetostructural transition.

DOI: [10.1103/PhysRevB.81.224406](https://doi.org/10.1103/PhysRevB.81.224406)

PACS number(s): 75.70.-i, 75.75.-c, 81.16.-c, 81.07.-b

I. INTRODUCTION

The further miniaturization demand in electronic devices requires a revision of the physical properties of their constituent materials. Particularly, in thin films the properties can be strongly modified respect to the bulk by two main factors: size effects and interfacial strain. Besides the well-known size effects, where quantum, interface, and surface effects become important, much attention is being paid nowadays to the strain effects arising from the crystalline misfit at the interface. Furthermore, as a consequence of its technological implication, these effects are gathered in a very active field called strain engineering, whose goal is to reach the desired properties by handling the film strain.^{1,2}

This work is focused on MnAs/GaAs(001) thin films, which from a technological point of view are interesting for hybrid metal/semiconductor spintronics, particularly concerning the use of the MnAs as a spin injector into semiconductors³. In these films the strain introduced by the epitaxy leads to very different physical properties compared to the bulk ones.^{4,5} On the one hand, the bulk MnAs has a first-order phase transition at $T_c=313$ K that drives the system from the hexagonal ferromagnetic phase (α) to an orthorhombically distorted paramagnetic phase (β).⁶⁻⁸ On the other hand, in the thin films epitaxially deposited on GaAs, the α and β phases coexist in a wide temperature range below T_c , that depends on the growth conditions.⁴ This is a consequence of the balance between the free energy released at the phase transition and the strain energy arising from the lattice and thermal mismatch between MnAs and GaAs.^{9,10} At the $\alpha \rightarrow \beta$ transition the hexagonal base of the crystalline structure shrinks anisotropically (Fig. 1) with a $\sim 1.2\%$ lattice-parameter discontinuity while the height of the prism remains unchanged.^{6,7} In the case of MnAs/GaAs(001), the anisotropic strain arising from the

α/β phase transition produces the characteristic alternating ridges and grooves stripes pattern along the MnAs [0001] direction.¹¹⁻¹³ Magnetic force microscopy (MFM) studies indicate that the ridges correspond to the ferromagnetic α phase and the grooves to the paramagnetic β one.¹⁴ The period λ of these stripes is determined by the MnAs layer thickness.^{10,15} For a given thickness, the relative α/β width ratio is determined by the temperature within the coexistence regime.

In this paper, we report on lateral size effects in the α/β phase coexistence as well as in the magnetic domains structure. MnAs/GaAs(001) epitaxial films were lithographed into ribbons so as to tailor a system where size and strain effects interplay. The lateral confinement effects are studied for different sizes: larger, comparable, and smaller than the period λ of the stripes array. The longest side of the ribbons was

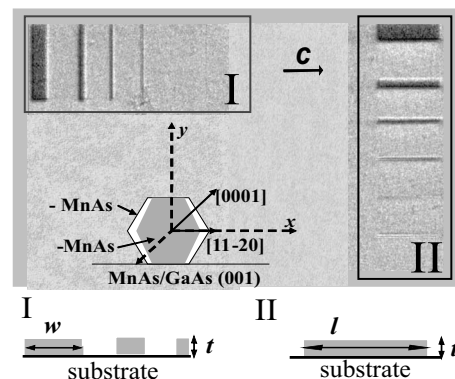


FIG. 1. MnAs ribbons made by e-beam lithography followed by Ar-ion milling. The ribbons are oriented (I) parallel and (II) perpendicular to the crystallographic c axis of the hexagonal lattice. Inset: schema of the MnAs/GaAs(001) epitaxy and shaded in gray the shrink of the hexagonal base during the $\alpha \rightarrow \beta$ transition is depicted.

oriented parallel and perpendicular to the MnAs[0001] crystallographic axis in the plane of the film. Structural and magnetic size effects in both directions were studied by atomic and magnetic force microscopy and explained in terms of the stress induced by the substrate and the magnetocrystalline anisotropy.

II. EXPERIMENT

The 150-nm-thick MnAs films were grown by molecular-beam epitaxy on a GaAs (001) substrate as described elsewhere.¹⁶ As the top surface of the microstructured ribbons was too rough (due to the patterning process) to study their topography by atomic force microscopy images, we exploited the fact that one of the coexisting phases is ferromagnetic and the other one, paramagnetic. Hence, we studied the phase coexistence by its magnetic contrast using the MFM technique. As the MFM setup is sensitive to the gradient of the magnetic force in the vertical direction, the bright and dark contrast in the MFM images correspond to places where the magnetic fields points out of or toward the surface plane, as described in Ref. 13. The images showed in this work were taken at room temperature in the remnant state after magnetizing the sample in a magnetic field of 1 T along the easy $[11\bar{2}0]$ magnetization direction.¹⁶

Two sets of MnAs ribbons were designed in order to study the dependence of the α/β phase coexistence on size and crystallographic orientation. The ribbons widths, w , were chosen in reference to the period of the α/β stripes array in the MnAs films ($\lambda_e \approx 4.8t = 0.72 \mu\text{m}$ for the present sample¹⁴). So we fabricated $2 \leq w \leq 5 \mu\text{m}$ ribbons larger than λ_e ; others with $0.5 \leq w \leq 1 \mu\text{m}$ comparable to λ_e ; and $0.1 \leq w \leq 0.2 \mu\text{m}$ ribbons smaller than λ_e (Fig. 1). The ribbons were arranged into two groups perpendicular to each other. The samples were carefully aligned in order to confine the films in the MnAs [0001] direction (I) and in the $[11\bar{2}0]$ direction (II) (Fig. 1).

In the first case the film stripes pattern is across the longest length of the ribbon while in the second case the stripes pattern lies along the ribbon. The length of the ribbons was fixed to $l = 20 \mu\text{m}$ while the spacing between them has been set to $10 \mu\text{m}$ in order to avoid dipolar magnetic interactions among them.

III. RESULTS AND ANALYSIS

The magnetic characterization of the as-cast film before microstructuration showed the typical behavior of these kind of films, as described in Refs. 16 and 17. The MFM characterization of the film at room temperature shows the typical stripes array for a MnAs/GaAs(001) film. The period measured for these stripes was $\lambda_m \sim 0.74 \mu\text{m}$, in excellent agreement with the estimated value, λ_e .¹⁴

Figure 2 shows MFM images obtained from MnAs ribbons confined along the [0001] direction (I). The images show the characteristic stripes pattern observed in thin films with the ferromagnetic α phase in the remnant state. The stripes configuration is preserved even for the smallest observed ribbon that has a width of $0.1 \mu\text{m} \ll \lambda_m$.

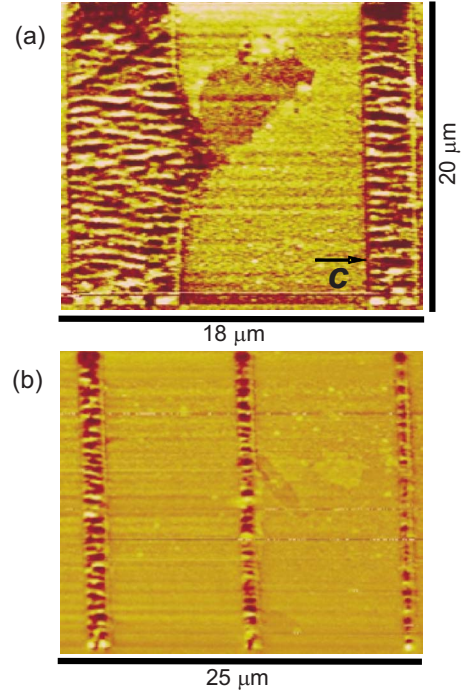


FIG. 2. (Color online) MFM images of the ribbons confined in the [0001] direction with widths of (a) 5 and 2 μm , and (b) 1, 0.5, and 0.2 μm .

Nevertheless, the phase coexistence is completely altered for the ribbons confined in the $[11\bar{2}0]$ direction (II). The 5 μm ribbon [Fig. 3(a)] shows the α/β stripes array running along the major direction of the ribbon [0001], copying the behavior of the thin MnAs film. The α stripes are saturated along the easy-magnetization direction, and the regions with dark/bright contrast indicate the stripes poles, with the stray field pointing in and out of the plane of the sample.

In the 2 μm width ribbon [Fig. 3(b)], the size effects become noticeable both in the structure and in the magnetic properties. Although the structure shows the coexistence of both α and β phases, the magnetic contrast suggests that they are not arranged in a regular stripes array of $\lambda_m \leq 0.74 \mu\text{m}$. In fact, for this regular array we would expect three periods in a 2 μm ribbon. Instead, only three different zones are clearly distinguishable from Fig. 3, still running along the [0001] direction. The remanence ratio, M_r/M_s , is smaller than 1, i.e., the α phase is not saturated at zero field and stripe-shaped domains are no longer observed along the c direction. At the edges of the ribbons, in areas of about $0.55(5) \mu\text{m}$ width, there is an intense magnetic contrast while in the central region a weaker magnetic contrast is observed. The magnetization of the borders is split into domains, arranged antiparallel between them with a periodicity of $\sim 1.8 \mu\text{m}$. A parallel alignment of neighbor domains, i.e., along the $[11\bar{2}0]$ direction, is also observed in the figure. This result can be explained in terms of magnetostatic interactions that couple the α ferromagnetic domains through the β zone. The whole domain configuration agrees with the analytical model proposed by Engel-Herbert and Hesjedal in Ref. 18

As schematized in the inset of Fig. 3(b), there would be α zones at the borders of the ribbons while the center would

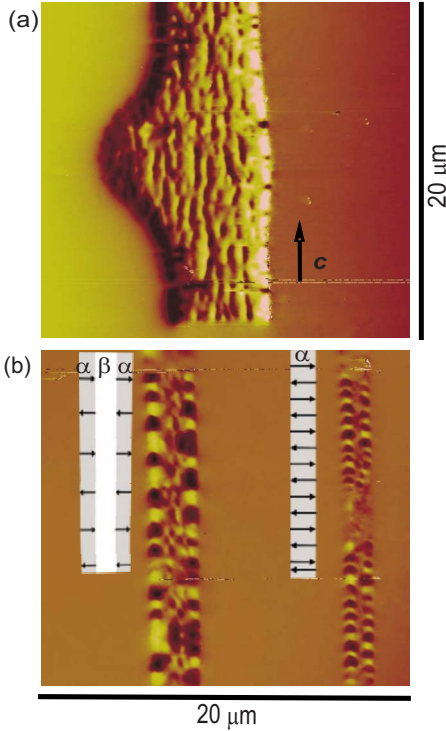


FIG. 3. (Color online) MFM images of the ribbons confined in the $[11\bar{2}0]$ direction with sizes of (a) $5\ \mu\text{m} \times 20\ \mu\text{m}$, (b) $2\ \mu\text{m}$ and $1\ \mu\text{m} \times 20\ \mu\text{m}$. The squared area highlights the parallel alignment of neighbor domains along the $[11\bar{2}0]$ direction. A schematic representation of the magnetic domain configurations of the 2 and 1 μm ribbons is also presented.

remain β . The α phase would be located at the borders of the ribbon due to stress relaxation at the side walls.^{19,20} The center of the ribbon is still kept under stress by the substrate, stabilizing the β phase.

As was highlighted before, there is an important difference of magnetic contrast along the $[11\bar{2}0]$ direction, being weaker at the center of the ribbons. We associate the brighter and darker areas at the borders of the ribbons to surface and constraint effects. In fact, additional magnetic anisotropy terms, arising from the ribbons roughness and strains, would induce a tilt of the magnetization of the external edges (lateral exposed walls) of the α zones out of the plane of the films. The stray fields produced by perpendicularly magnetized zones are more intense leading to brighter/darker spots.

The width of the 1 μm ribbon [Fig. 3(b)] is comparable to the λ_m period. In this case, too, the remanence ratio is less than 1 suggesting a strong demagnetizing size effect; i.e., the magnetization of the sample is split into domains of alternate polarity along the c axis.

In the 1 μm ribbon, there is an alternated sequence of antiparallel domains along the c axis and magnetized in the $[11\bar{2}0]$ direction. The domain period along the $[0001]$ direction is $\sim 0.85\ \mu\text{m}$, much shorter than the one measured in the 2 μm ribbon. The MFM picture [Fig. 3(b)] shows almost no contrast in the middle of the ribbon and dark/bright spots at its borders, perpendicular to the $[11\bar{2}0]$ direction. The magnetic contrast indicates that the samples surface is single

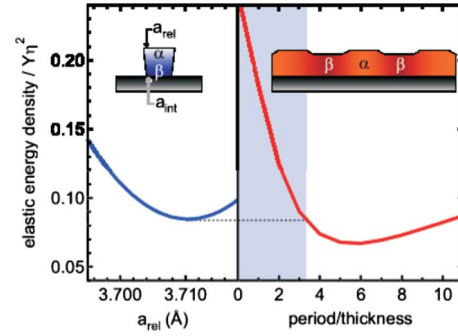


FIG. 4. (Color online) Left: elastic energy density of a ribbon allowed to adjust its parameter along the direction normal to the substrate from a_{int} to a_{rel} . Right: elastic energy density of the α - β stripes pattern as a function of its period scaled over thickness of the epilayer.

phase and ferromagnetic, magnetized in the plane of the substrate, with the stray fields pointing in/out the ferromagnetic surface. We consider that the stress-free walls could not be in the β phase at room temperature, i.e.,²¹ below the Curie temperature. In this case, as reported in Refs. 20 and 21 for disks having their diameter sizes comparable to the stripes period of the former films, the α phase is in the surface of the disk, while the β one lies inside of it (at GaAs interface), kept under stress by the substrate.

So, while the system confined in the MnAs $[0001]$ direction showed mainly the same structural and magnetic properties as the unconfined film, ribbons confined along the $[11\bar{2}0]$ direction present remarkable size effects. In this orientation, the configuration of elastic domains in stripes is preserved only for ribbons broader than 2 μm . Although the two phases still coexist for 2 μm ribbons, the array of the α and β domains is notably changed.

Kaganer *et al.*^{10,22} modeled the α -MnAs- β -MnAs phase coexistence in MnAs thin films. In their model, the constraint imposed by GaAs substrate on the MnAs film is the key for explaining this phenomenon. The fact that the size of the films is restricted to the substrate size makes the mean total strain on the MnAs film plane equal to zero and as a consequence, an additional elastic energy term arises. A phase coexistence is thus developed at the first-order transition of bulk MnAs in order to minimize the total elastic energy. Due to the fact that the structural transition is also accompanied by a lattice-parameter discontinuity at the hexagonal plane, the configuration of the elastic domains is highly anisotropic. From Kaganer *et al.*, the elastic energy density of the pattern (the period λ_e of the α - β pattern is $2\lambda t$, where t is the epilayer thickness), for equal α - β fraction, is given by

$$E_d = 2Y\eta^2 \sum_{n=1}^{\infty} \left[1 - \frac{2\lambda}{\pi n} (1 - e^{-\pi n/\lambda})^2 \right] \frac{\sin^2(\pi n/2)}{(\pi n)^2}, \quad (1)$$

η is the α - β phase transition strain and Y the Young modulus. From Eq. (1) it is possible to compute the elastic energy as a function of λ_e/t . The resulting curve is given in Fig. 4.

Considering a ribbon cut transversally to the stripes direction, it is possible to compute the elastic energy density for

strain distributions other than stripes. Indeed, due to finite size, edge relaxation may occur. At equal α - β fraction, a simple distribution is a linear variation in the lattice parameter in the a direction from a_{int} , the lattice parameter in the vicinity of the substrate, to a_{rel} close to the epilayer surface. Neglecting strain along the c axis, it is then straightforward to calculate E_{ribbon} the elastic energy density resulting from such a distribution. We obtain a minimum for a_{rel} close to a_{α} ,²³ which indicates that it is energetically favorable for a finite-size structure to have the α phase in the surface and the β one underneath.

Then, from Fig. 4, it is straightforward to conclude that for ribbons having a width smaller than $\sim 3.2t$, the relaxation through stripes pattern formation is no longer the most efficient channel. Of course, the strain distribution chosen here is certainly a crude approximation and the real one could be more subtle and remains to be determined. However, this simple model illustrates how size reduction affects the channel followed by the system to relax its elastic energy. We also note that the simple distribution considered here for the strain at equal phase fraction implies that MnAs is actually strained in the whole ribbon: the real distribution may lead to further energy minimization and stripes disappearance may occur for ribbons having a width above $3.2t$. Another key point has to be considered: Eq. (1) gives the elastic energy density per domain for an infinite pattern. There are no consideration on the borders. For small ribbons with a width equal to a few times the thickness, the situation is between infinite pattern (stripes favored) and very small ribbon for which stripes are not favored. In this range, the period is unlikely to take the value giving the minimal value of E_d : boundary conditions at the border of the ribbon have to be taken into account. For example, β -MnAs will not be favored at the edges. Therefore, the stripes pattern will not adjust its period to $\lambda_e = 4.8t$ in this case and may not be the most stable elastic state. This explains the disappearance of the pattern for a ribbon of 2 μm width and 150 nm thickness.

As seen, both confinement directions show differences in the magnetic properties, too. On the one hand, for the system confined in the MnAs [0001] direction the magnetic properties are only slightly disturbed, as the system is confined perpendicular to the easy-magnetization direction. In this

case the ferromagnetic coupling between neighbor stripes remains unchanged, leading to a rather small demagnetizing field and there are not noticeable size effects in the magnetization. On the other hand, ribbons confined along the easy-magnetization direction preserve their magnetic properties undisturbed as long as the lateral dimensions of the system are enough to ensure that the magnetocrystalline anisotropy is stronger than the demagnetizing field. When lowering the lateral dimensions ($w \leq 2 \mu\text{m}$) size effects become important and the demagnetizing field due to the uncompensated phase in the borders tends to demagnetize the system and favor the antiferromagnetic coupling between adjacent magnetic domains. This effect is more noticeable as the size is lowered in the $[11\bar{2}0]$ direction, as we showed comparing the 2 and 1 μm ribbons.

IV. CONCLUSION

In summary, we report a systematic study of lateral and directional confinement effects on MnAs/GaAs(001) microscopic ribbons. Different structural and magnetic effects are observed when confining the system along the mutually perpendicular [0001] and $[11\bar{2}0]$ directions. While the structural and magnetic properties of the ribbons remain unchanged when they major axis are oriented perpendicular to the [0001] direction, strong size effects are observed in the ribbons confined in the $[11\bar{2}0]$ direction. In the last samples, we have observed a reorganization of the phase coexistence array and a decrease in the remnant magnetization when the lateral sizes of the ribbons are comparable to the stripe period λ_e . This behavior is explained in terms of strain effects due to the volume change during the phase transition. Our results evidenced the critical role of size and designs orientation in the magnetostructural properties of microscopic MnAs/GaAs(001)-based devices.

ACKNOWLEDGMENTS

We acknowledge the partial financial support from PICT 33304 and CONICET PIP 1333. We also acknowledge H. Pastoriza for the use of the microfabrication facilities. M.T. wish to thank Lic. C. von Bilderling for the technical support at the CMA FCEyN, UBA.

¹Y. Kato, R. C. Myers, A. C. Gossard, and D. D. Awschalom, *Nature (London)* **427**, 50 (2004).

²D. H. Mosca, F. Vidal, and V. H. Etgens, *Phys. Rev. Lett.* **101**, 125503 (2008).

³V. Garcia, H. Jaffres, M. Eddrief, M. Marangolo, V. H. Etgens, and J. M. George, *Phys. Rev. B* **72**, 081303(R) (2005).

⁴N. Mattoso, M. Eddrief, J. Varalda, A. Ouerghi, D. Demaille, V. H. Etgens, and Y. Garreau, *Phys. Rev. B* **70**, 115324 (2004).

⁵A. K. Das, C. Pampuch, A. Ney, T. Hesjedal, L. Däweritz, R. Koch, and K. H. Ploog, *Phys. Rev. Lett.* **91**, 087203 (2003).

⁶R. H. Wilson and J. S. Kasper, *Acta Crystallogr.* **17**, 95 (1964).

⁷B. T. M. Willis and H. Rooksby, *Proc. Phys. Soc. London, Sect.*

B **67**, 290 (1954).

⁸J. B. Goodenough and J. A. Kafalas, *Phys. Rev.* **157**, 389 (1967).

⁹F. Iikawa, P. V. Santos, M. Kästner, F. Schippan, and L. Däweritz, *Phys. Rev. B* **65**, 205328 (2002).

¹⁰V. M. Kaganer, B. Jenichen, F. Schippan, W. Braun, L. Däweritz, and K. H. Ploog, *Phys. Rev. B* **66**, 045305 (2002).

¹¹T. Plake, M. Ramsteiner, V. M. Kaganer, B. Jenichen, M. Kästner, L. Däweritz, and K. H. Ploog, *Appl. Phys. Lett.* **80**, 2523 (2002).

¹²M. Kästner, C. Herrmann, L. Däweritz, and K. H. Ploog, *J. Appl. Phys.* **92**, 5711 (2002).

¹³F. Schippan, G. Behme, L. Däweritz, K. H. Ploog, B. Dennis,

- K.-U. Neumann, and K. R. A. Ziebeck, *J. Appl. Phys.* **88**, 2766 (2000).
- ¹⁴L. Däweritz, L. Wan, B. Jenichen, C. Herrmann, J. Mohanty, A. Trampert, and K. H. Ploog, *J. Appl. Phys.* **96**, 5056 (2004).
- ¹⁵L. Däweritz *et al.*, *J. Cryst. Growth* **227**, 834 (2001).
- ¹⁶L. B. Steren, J. Milano, V. Garcia, M. Marangolo, M. Eddrief, and V. H. Etgens, *Phys. Rev. B* **74**, 144402 (2006).
- ¹⁷L. Däweritz, *Rep. Prog. Phys.* **69**, 2581 (2006).
- ¹⁸R. Engel-Herbert and T. Hesjedal, *Phys. Rev. B* **78**, 235309 (2008).
- ¹⁹Y.-H. Yoo, W. Lee, and H. Shin, *Semicond. Sci. Technol.* **19**, 93 (2004).
- ²⁰Y. Takagaki, B. Jenichen, C. Herrmann, E. Wiebicke, L. Däweritz, and K. H. Ploog, *Phys. Rev. B* **73**, 125324 (2006).
- ²¹J. Mohanty, T. Hesjedal, A. Ney, Y. Takagaki, R. Koch, L. Däweritz, and K. H. Ploog, *Appl. Phys. Lett.* **83**, 2829 (2003).
- ²²V. M. Kaganer, B. Jenichen, F. Schippan, W. Braun, L. Däweritz, and K. H. Ploog, *Phys. Rev. Lett.* **85**, 341 (2000).
- ²³C. Adriano, C. Giles, O. D. D. Couto, M. J. S. P. Brasil, F. Iikawa, and L. Däweritz, *Appl. Phys. Lett.* **88**, 151906 (2006).